

# Automated Docking to Multiple Target Structures: Incorporation of Protein Mobility and Structural Water Heterogeneity in AutoDock

Fredrik Österberg, Garrett M. Morris, Michel F. Sanner, Arthur J. Olson, and David S. Goodsell\*

*Department of Molecular Biology, Scripps Research Institute, La Jolla, California*

**ABSTRACT** Protein motion and heterogeneity of structural waters are approximated in ligand-docking simulations, using an ensemble of protein structures. Four methods of combining multiple target structures within a single grid-based lookup table of interaction energies are tested. The method is evaluated using complexes of 21 peptidomimetic inhibitors with human immunodeficiency virus type 1 (HIV-1) protease. Several of these structures show motion of an arginine residue, which is essential for binding of large inhibitors. A structural water is also present in 20 of the structures, but it must be absent in the remaining one for proper binding. Mean and minimum methods perform poorly, but two weighted average methods permit consistent and accurate ligand docking, using a single grid representation of the target protein structures. *Proteins* 2002;46:34–40. © 2001 Wiley-Liss, Inc.

**Key words:** protein flexibility; peptidomimetic inhibitors; HIV-1;

## INTRODUCTION

Protein flexibility is a major hurdle facing automated docking. Effective methods are available for docking a flexible ligand to a rigid target, permitting large ligands on the order of hexapeptides to be docked reliably and quickly.<sup>1,2</sup> In our experience, these methods are effective for approximately one-half of the systems presented to them. These are cases in which the protein target is relatively rigid and the crystallographic structure of protein, solved either alone or in complex with a given ligand, is an adequate representation of the conformation of the protein in the desired docked complex.

Many systems, however, show significant motion upon binding to ligands.<sup>3</sup> This motion often involves local rearrangement of side-chains or small motions of loops. These small motions, however, have a great effect on docking results, often spelling the difference between success and failure.<sup>4</sup>

Docking simulations with a fully flexible target currently are not feasible, given the need to obtain a docked result with a computational effort of minutes. For instance, Apostolakis and coworkers<sup>5</sup> have reported a Monte Carlo docking method that permits full flexibility of the protein target. The method was successful on an antibody complex that required protein motion for proper docking, but required several days of computation to obtain the

result. By contrast, many methods have been reported for simplifying the molecular description, allowing incorporation of a limited model of protein motion while keeping computational times to a minimum. Examples include, for instance, models that treat selected side-chains as flexible,<sup>6,7</sup> models that use a small set of rotomers,<sup>8,9</sup> hierarchical approaches that treat side-chain flexibility after roughly docked positions have been found,<sup>10</sup> and methods that treat larger motions using harmonic modes<sup>11</sup> or hinged domains.<sup>12</sup>

This article explores methods for combining several three-dimensional structures, which cover a range of motion of side-chains and loops, into a single docking simulation. This incorporates protein motion into the docking simulation, while introducing only moderate increases in the computational expense. The work extends previously reported work, using the DOCK method,<sup>13</sup> in which multiple structures were combined in a pairwise-atom energy evaluation.

The AutoDock 3.0 package of software is used for docking simulation.<sup>14</sup> AutoDock uses a rapid grid-based lookup method for energy evaluation. The use of interaction energy grids allows the use of a sophisticated empirical free energy force field, while greatly reducing the computational demands of the docking simulation. However, the grid-based method currently limits AutoDock to a rigid model for the target protein. The problem explored is to define methods for combining several protein structures into a single representative grid of interaction energies. The resulting methods are effective for incorporation of side-chain motion into docking simulations and are also successful in a case in which structural waters show heterogeneity in different complexes.

We have tested these methods on HIV-1 protease, an important medicinal target.<sup>15,16</sup> HIV-1 protease shows the type of flexibility that can pose significant problems in docking simulation. The active site is lined with flexible residues that adopt different conformations, allowing the protein to recognize and cleave a variety of peptide sub-

Grant sponsor: National Institutes of Health; Grant number: P01 GM48870.

\*Correspondence to: David S. Goodsell, Department of Molecular Biology, Scripps Research Institute, 10550 North Torrey Pines Road, La Jolla, CA 92037. E-mail: goodsell@scripps.edu

Received 5 April 2001; Accepted 21 August 2001

strates. Numerous crystallographic structures are available (see the HIV Protease Database at <http://www.ncicrf.gov/HIVdb>), which provide snapshots of the various conformations available within the active site. In this work, we have tested the methods on 21 complexes of HIV-1 protease with diverse inhibitors, shown in Figure 1. Twenty of these inhibitors rely on a structural water for stability, and one inhibitor displaces this water, requiring that the water site be empty for binding. Ideally, we are seeking a method that incorporates both the variations in protein conformation and the variations in water structure, which would allow prediction of binding conformations for all 21 inhibitors using a single, combined target representation.

Note that HIV-1 protease also undergoes a massive rearrangement of two flaps during association with the substrate. The methods described will not be effective for this type of large rearrangement. These methods are designed for incorporation of smaller (but critical) motions of side-chains like those observed in the many complexed HIV-1 protease structures.

## METHODS

### Calculation of Combined Interaction Energy Grids from Multiple Structures

Grids of interaction energy are calculated by placing a probe atom at discrete points in the space around the target protein and assigning to the grid point the value of the interaction energy between the probe and the surrounding protein atoms. This grid of interaction energy values may then be used as a lookup table to speed docking simulations, requiring a simple interpolation instead of the many pairwise atomic calculations for each sample ligand conformation. These grids are dominated by the repulsive areas occupied by the target protein atoms, which have large positive values, within the range of 0–10,000 kcal/mol. The surrounding accessible regions have weakly favorable values, having negative values of a few kcal/mol.

Given several different structures of a target protein that have differences in protein conformation or water structure, one can imagine calculating grids of interaction energies for each and then combining the grids into one for use in docking. Two simple methods come to mind first. A mean grid takes a simple point-by-point average across all the grids, and a minimum grid takes the minimum value across all the grids. The effect of each may be seen in Figure 2(a,b). In the mean map, the repulsive areas (in red) dominate. If any map has a large positive energy at a given point, it will force the mean to have a repulsive energy. As we will see below, this is far too restrictive. The minimum map addresses this problem. It shows repulsive areas only when all the maps have large energies. However, it overestimates the favorable regions of the map.

We have explored two methods for weighting the grids that address the limitations of average and minimum grids. The first is a modification of the method presented by Knetgel et al.,<sup>13</sup> which we term a clamped grid. A weighted average of the energies across all the structures is computed at each point. For each structure, the weight

is given a value of 1 if the interaction energy of the point is less than a given threshold, which was taken to be 0 kcal/mol in this case. If the energy is greater than the threshold, a very small weight of 0.0001 is applied. Then when the average is taken, the weights are normalized to give a sum of 1.

This weighting scheme has a desirable effect. If one or more of the grids contain a favorable, negative value, their weights will dominate the average, and the grid point will have a favorable energy. If, however, all the grids contain unfavorable positive values, all will have identical weights of 0.0001, so the average will yield an unfavorable, positive value that reflects all the grids. In the report by Knetgel et al.<sup>13</sup>, the weighted average was performed at the time that pairwise energies were calculated, rather than after interaction energy grids were calculated. A ramping scheme was also used to assign intermediate values between the two different weights. An example of a clamped map is shown in Figure 2(c).

The artificial nature of the clamped weighting scheme, with its arbitrary thresholds, is improved in a second scheme, which we term an energy-weighted grid. This is a similar approach to the clamped average, but uses a Boltzmann assumption to calculate the weight ( $W$ ) based on the interaction energy ( $\Delta G$ ):

$$W = \exp(-\Delta G/RT)$$

As before, the weights are normalized when the average is taken. This function has all the desirable properties of the clamped method, but with a sounder physical justification. At equilibrium, a collection of protein–ligand complexes will be found in quantities that are related to the energy of interaction. Here, we calculate the “combined” energy as an average of the energies of each individual conformation, weighted by how often we would expect to find them in the ensemble. Figure 2(d) presents an example of an energy-weighted map.

### Automated Docking

To test the combined grids, we used a test set of 21 HIV-1 protease complexes, listed in Figure 1. This set includes a diverse collection of inhibitors, ranging in size, flexibility, and chemical content. For each protein structure, the ligand was removed, polar hydrogen atoms were added geometrically, and Kollman united-atom charges<sup>17</sup> were assigned in Sybyl (Tripos). The water coordinated under the flaps (301, in most cases) was retained, except in the case of 1hvr, which does not bind a water molecule in this position. The protein coordinates were superimposed using the alpha carbon ( $C\alpha$ ) atoms and structure 4hvp as the reference. Grids were then calculated for each protein individually, using a grid spacing of 0.375 Å. Combined grids were then calculated using the four methods described above.

Docking experiments were performed with flexible side-chains in each ligand, but holding the main-chain rigid in the crystallographic conformation. Hydrogen atoms were added geometrically to ligands and charges added by the Gasteiger–Marsili method<sup>18</sup> in Sybyl (Tripos). Ligands

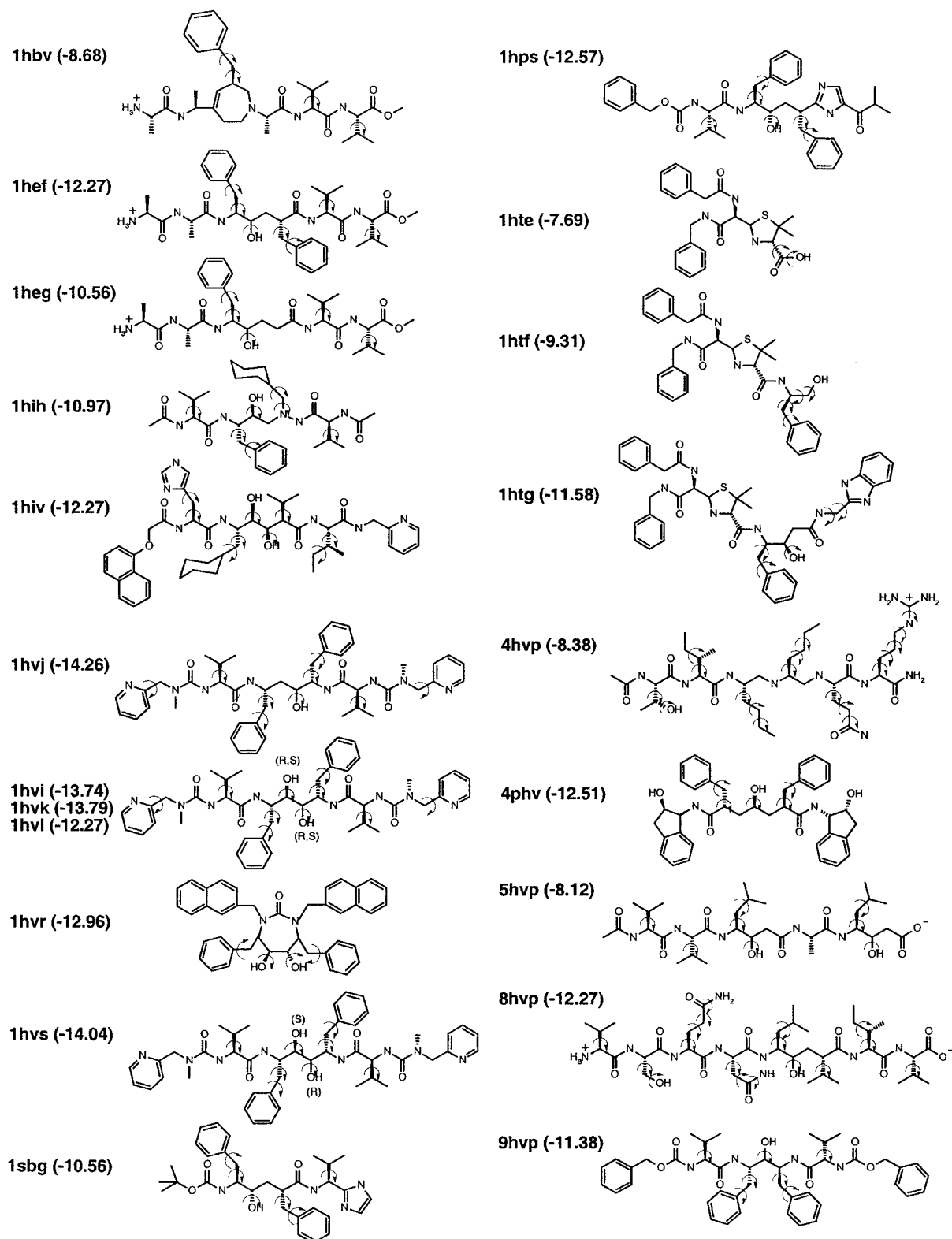


Fig. 1. Ligands bound to human immunodeficiency virus type 1 (HIV-1) protease in the 21 complexes tested in this work. Coordinates for each complex were obtained from the Protein Data Bank (<http://www.pdb.org>), using the accession codes given here. Bonds that were treated as flexible are indicated by curly arrows. Note that structures 1hvi, 1hvk, and 1hvl differ only in the stereochemistry of the non-scissile bond and are shown with one structure. Experimental free energies of binding (in kcal/mol) are also given in parentheses; they were obtained from the primary reference for each crystallographic structure.

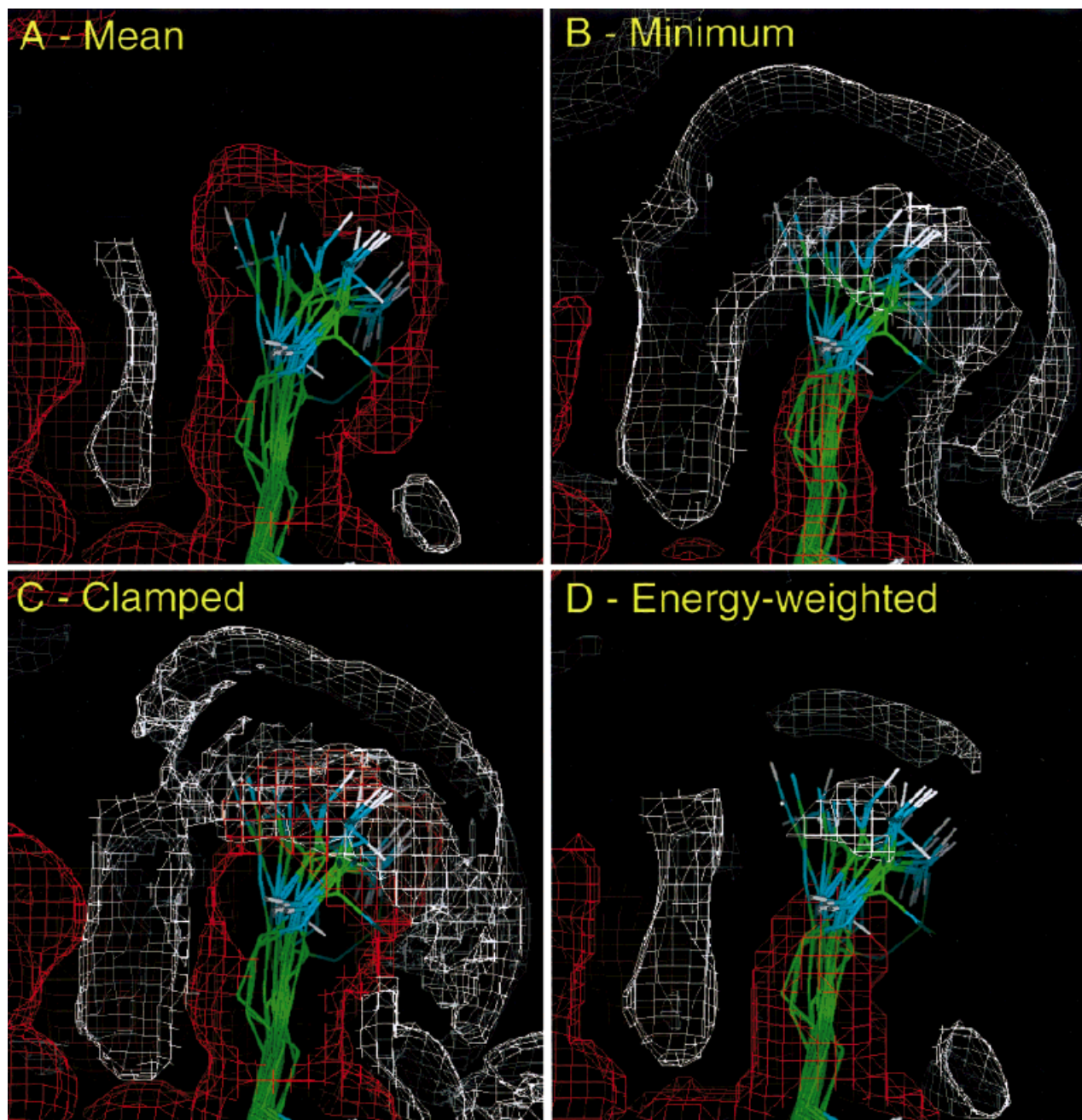


Fig. 2. Combined maps of oxygen interaction energy: (a) mean, (b) minimum, (c) clamped, and (d) energy-weighted. In each case, 21 protein structures are combined into a single map, and the view is centered on Arg8, which shows significant motion. Strong repulsive energies are shown in red at a contour level of 250 kcal/mol; favorable peaks are shown in white at a contour level of  $-0.1$  kcal/mol. The mean map is dominated by the repulsive energies, which surround the entire collection. The minimum map confines the repulsive region to areas occupied by protein atoms in all the structures, and a smeared halo of favorable energy corresponding to all the hydrogen-bonding positions. The two weighted maps at the bottom are intermediate between these extremes, showing unfavorable contours for regions that are most occupied by protein atoms, and weighting particular hydrogen-bonding sites strongly if many structures contribute to the site.

were then prepared with the AutoTors utility of AutoDock, to remove the nonpolar hydrogen atoms and unite their charges with the bonded carbon atom, and to assign aromatic carbon atoms. Docking was performed using the Lamarkian genetic algorithm in AutoDock 3.0. Each docking experiment was performed 10 times, yielding 10 docked conformations. Parameters for the docking are as

follows: population size of 10; random starting position and conformation; maximal mutation of 2 Å in translation and 50 degrees in rotations; elitism of 1; mutation rate of 0.02 and crossover rate of 0.8; and local search rate of 0.06. Simulations were performed with a maximum of 1.5 million energy evaluations and a maximum of 27,000 generations. Final docked conformations were clustered



**TABLE I. Correlation of Experimental and Predicted Binding Free Energies**

	Slope	<i>R</i>	RMSD in energies (kcal/mol)
Redocked	0.95	0.75	1.43
Mean	0.46	0.43	7.69
Minimum	1.50	0.76	6.07
Clamped	1.04	0.79	1.34
Boltzmann	0.95	0.75	1.43

Least-squares fitting was performed across all 21 ligands, by forcing the line to pass through the origin. Slope and residual *R*-value are presented. The root-mean-square deviation is calculated between experimental and predicted binding free energies in each set.

using a tolerance of 1 Å root-mean-square deviation (RMSD). For a full explanation of these parameters, please refer to the report of AutoDock 3.0.<sup>14</sup>

## RESULTS AND DISCUSSION

### Automated Docking to Single Target Structures

To evaluate the need for methods to combine multiple target structures of a target protein, we first tested our collection of complexes individually in a cross-docking experiment. Each of the 21 ligands was docked to each of the 21 protein structures, yielding a matrix of 441 docked complexes. We would expect the complexes along the diagonal of this matrix—redocked complexes—to match the crystallographic conformations, and to give good prediction of the free energy of association, since any “induced fit” due to the inhibitor will be present in the protein conformation. In 19 of 21 complexes, this is the case, as shown in Table I. The RMSD between the predicted free energies and the reported free energies is 1.70 kcal/mol, well within the tolerance of 3 kcal/mol identified in previous reports of AutoDock. The conformation of lowest energy was within 2.2 Å RMSD of the observed structure. Docking was consistent as well, with an average of 7.5 of the 10 docked structures clustered close to the crystallographic conformation.

The remaining two structures, 1hte and 1htf, showed high RMSD for the conformation of lowest energy. For 1htf, if the two conformations of lowest energy are transformed around the twofold axis relating the two protease subunits, they then superimpose with the crystallographic conformation with RMSD of 1.25 Å. The remaining eight predicted conformations all superimpose with the crystallographic conformation with RMSD less than 0.75 Å. In the structure 1hte, the small inhibitor fills only one-half of the active site, and there is a second molecule filling the remainder of the active site, which is not modeled in our simulation. The top two predicted conformations are improperly docked, with RMSD of >6 Å and predicted free energy of −11.07 kcal/mol. The remaining eight conformations are identical to the crystallographic conformation, with RMSD within the range of 0.94–1.04 Å and energies only 1 kcal/mol less favorable than the top two misdocked conformations, with energies within the range of −10.20 to −10.24 kcal/mol.

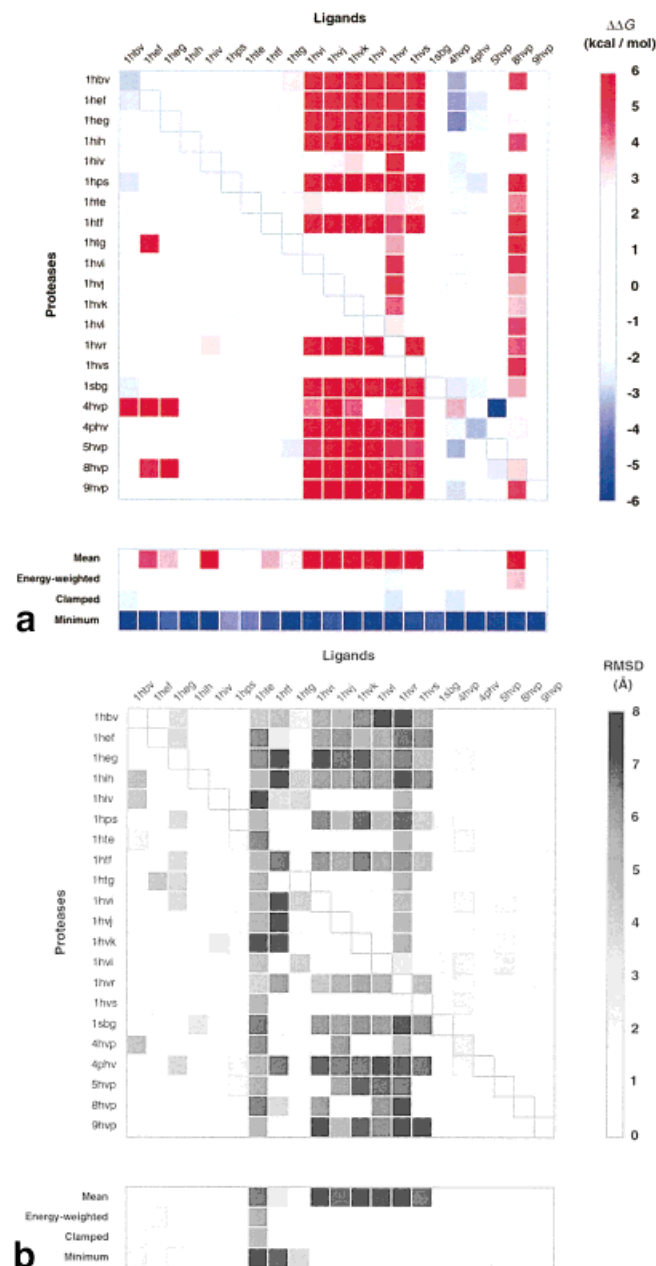


**Fig. 3.** Results of docking simulations. The upper portion shows that each of the 21 ligands is docked to each of the 21 protein structures. In the lower portion, each ligand is docked to the four combined maps. **a:** Difference between docked binding free energies and the experimental binding free energies. **b:** Root-mean-square deviations (RMSD) in coordinates between the docked conformation of most favorable energy and the crystallographic conformation.

Many of the off-diagonal, cross-docking experiments also gave excellent results, as seen in Figure 3. Thirteen of the ligands showed reasonable docked energies and RMSD to the experimental structure when docked to any of the protein structures. The remaining inhibitors were far more sensitive to protein conformation, docking successfully to only a few of the protein structures. Similar cross-docking results have been reported using the incremental docking method FlexX<sup>19</sup> and the Tabu search in

PRO\_LEADS,<sup>4</sup> in which about one-half of the ligands were relatively insensitive to protein motion, and the other half required a very specific protein conformation for proper docking.

Five large inhibitors from files 1hvi, 1hvj, 1hvk, 1hvl, and 1hvs could only be docked to proteins taken from this same set of five complexes. These ligands could not be docked successfully to most of the other protein conformations in the test set, as indicated by the dark columns of values at the center of Figure 3. In these five structures, Arg8 is flipped outward from the active site by almost 2 Å, allowing extra room for the large ligands. In the other structures, Arg8 adopts a position that blocks binding. This is exactly the type of motion that we are seeking to accommodate in the averaged grids tested here.

The two small inhibitors in files 1hte and 1htf showed poor docking to the entire set of proteins. This is a consequence of the small size of the inhibitors and of the large size of the protease active site. AutoDock found many conformations of approximately equal energy.

Finally, the structure of a cyclic urea inhibitor, from file 1hvr, shows the effect of heterogeneity in structural waters. In the crystal structure, the inhibitor displaces the structural water bound under the protease flaps (water 301). Unsurprisingly, this inhibitor was not effectively docked to any of the other protein structures, because of the presence of this water in the target model. However, docking of the other 20 inhibitors to the 1hvr protease structure, without water 301, showed good results, as seen in the row labeled 1hvr in Figure 3. The results are similar to the docking results obtained with the other 20 protein structures, which included water 301.

### Automated Docking to Combined Representations of Multiple Target Structures

Each of the 21 ligands was then docked to the four combined grids. The results are presented in the lower portion of Figure 3, and the correlation of predicted and observed free energies are presented in Table I.

The mean grids performed poorly. The overall prediction of binding energies was poor, with a poor correlation and poor RMSD between the predicted and experimental binding free energy values. Eight structures showed coordinate RMSD values of >2.0 Å. The performance on the five long ligands did not improve—all were docked incorrectly, showing high binding energies and poor RMSD relative to the crystallographic conformation. This is understandable, as the average map contains a union of all the repulsive areas. Thus, for Arg8, the repulsive area covers all the conformations, including the ones that exclude the large ligands. The cyclic urea inhibitor was also docked incorrectly, because the mean map includes the full steric effect of water 301 from 20 of the structures.

The minimum maps performed better, successfully finding docked conformations for all the ligands close to the crystallographic conformations. For three ligands—1hte, 1htf, and 1htg—one incorrectly docked conformation was found at the lowest energy. This was followed by a large cluster of conformations with RMSD of <2.0 Å and ener-

gies within 0.2 kcal/mol of the lowest energy. This observation, along with the fact that the overall RMSD for all the ligand conformations are higher than for the other map combination methods, indicates that the minimum method is losing specificity in docking, allowing a wider range of variation in the best conformations chosen. This is also reflected in the predicted free energies, which show a good correlation with observed values but are all several kcal/mol too low, as shown by the blue colors in Figure 3(a), and reflected in the high RMSD of experimental and predicted energies and slope of >1 (Table I). This is understandable, as the minimum maps overestimate the spatial extent of the favorable binding regions of the active site.

The two weighted maps performed very well. Both found good docked conformations with acceptable predicted free energies for all the ligands, with the exception of the small ligand in 1hte. For the five large ligands, these grids were able to soften the repulsion of Arg8, while maintaining an average of the favorable areas that reflected all the structures, instead of just the best. The cyclic urea inhibitor was also docked correctly, because the combined maps softened the repulsion of water 301 present in 20 of the 21 structures. At the same time, the other 20 inhibitors were also docked correctly, because the combined maps also retain an image of the hydrogen bonding interaction of this water. The RMSDs between experimental and predicted energies were quite good, at 1.43 and 1.34 kcal/mol for the energy-weighted and clamped methods respectively.

The robustness of docking, evaluated as the number of times the lowest-energy conformation was found in each set of 10 docking runs, varied from method to method. The averaged grids were the worst: over the 21 different ligands, docking to the averaged grids found the proper conformations in 38% of the simulations. The energy-weighted and clamped methods performed better, with 87% and 72% of the simulations finding the proper conformation. The minimum maps were also consistent, finding the proper conformation in 81% of the simulations. This is fully to be expected, since the minimum grids have larger regions of favorable energy, which might be expected to smooth the grids and promote search of the conformation space.

### CONCLUSIONS

By combining many structures into a single map of interaction energy, we are able to retain the speed available through use of energy lookup methods while incorporating a significant level of protein conformational and solvation diversity. Of course, a tradeoff in computational resources applies. The computational expense of combining multiple structures, either multiple crystallographic or NMR structures or snapshots from a molecular dynamics simulation, must be weighed against the computation time for a docking method that uses explicit protein flexibility. In cases in which multiple ligands are docked to a single protein target, as in a typical drug discovery program, the overhead for calculation of combined maps is not a problem.

The energy-weighted and clamped techniques are both good predictive methods for finding docked conformations with accurate free energies. Both showed good success in the incorporation of limited protein motion, such as the multiple conformations of Arg8 that confound one-third of the simulations when docked individually. Both methods also allowed multiple solvation models to be incorporated into a single docking simulation, as demonstrated by the docking of a cyclic urea inhibitor to a combined map derived from 20 structures both with and without water 301.

Finally, note that this method for incorporation of conformational and solvent diversity can introduce potentially dangerous artifacts. For instance, the combined oxygen maps include favorable peaks both for binding to water 301 and for binding in place of water 301. In the case of the inhibitors tested here, this is not a problem, as the molecules are designed in such a way that only one of the two options is exercised. For applications in which natural biological molecules are studied, such as binding of cofactors to enzymes or binding of proteins to receptors, we expect that this problem will be minimized, as these complexes will have been optimized by evolution to select one possible conformation and solvation state for binding. But during inhibitor design, it would be possible to create paradoxical inhibitors that bind to mutually exclusive combinations of features from different conformations.

## ACKNOWLEDGMENTS

The authors thank Ruth Huey for her assistance. This is manuscript 13686-MB from the Scripps Research Institute.

## REFERENCES

1. Rosenfeld R, Vajda S, DeLisi C. Flexible docking and design. *Annu Rev Biophys Biomol Struct* 1995;24:677–700.
2. Kuntz ID, Meng EC, Shoichet BK. Structure-based molecular design. *Acc Chem Res* 1994;27:117–123.
3. Najmanovich R, Kuttner J, Sobolev V, Edelman M. Side-chain flexibility in proteins upon ligand binding. *Proteins* 2000;39:261–268.
4. Murray CW, Baxter CA, Frenkel AD. The sensitivity of the results of molecular docking to induced fit effects: application to thrombin, thermolysin and neuraminidase. *J Comp-Aided Mol Design* 1999;13:547–562.
5. Apostolakis J, Pluckthun A, Caffisch A. Docking small ligands in flexible binding sites. *J Comp Chem* 1998;19:21–37.
6. Leach AR. Ligand docking to proteins with discrete side-chain flexibility. *J Mol Biol* 1994;235:345–356.
7. Jones G, Willett P, Glen RC. Molecular recognition of receptor sites using a genetic algorithm with a description of desolvation. *J Mol Biol* 1995;245:43–53.
8. Desmet J, Wilson IA, Joniau M, DeMaeyer M, Lasters I. Computation of the binding of fully flexible peptides to proteins with flexible side chains. *FASEB J* 1997;11:164–172.
9. Schaffer L, Verkhivker GM. Predicting structural effects in HIV-1 protease mutant complexes with flexible ligand docking and protein side-chain optimization. *Proteins* 1998;33:295–310.
10. Schnecke V, Swanson CA, Getzoff ED, Tainer JA, Kuhn LA. Screening a peptidyl database for potential ligands to proteins with side-chain flexibility. *Proteins* 1998;33:74–87.
11. Zacharias M, Sklenar H. Harmonic Modes as variables to approximately account for receptor flexibility in ligand-receptor docking simulations: application to DNA minor groove ligand complexes. *J Comp Chem* 1999;20:287–300.
12. Sandak B, Wolfson HJ, Nussinov R. Flexible docking allowing induced fit in proteins: insights from an open to closed conformational isomers. *Proteins* 1998;32:159–174.
13. Knegtel R, Kuntz I, Oshiro C. Molecular docking to ensembles of proteins. *J Mol Biol* 1997;266:424–440.
14. Morris GM, Goodsell DS, Halliday RS, Huey R, Hart WE, Belew RK, Olson AJ. Automated docking using a Lamarckian genetic algorithm and an empirical binding free energy function. *J Comp Chem* 1998;19:1639–1662.
15. Wlodawer A, Vondrasek J. Inhibitors of HIV-1 protease: a major success of structure-assisted drug design. *Annu Rev Biophys Biomol Struct* 1998;27:249–284.
16. Tomasselli A, Heinrikson RL. Targeting the HIV-protease in AIDS therapy: a current clinical perspective. *Biochim Biophys Acta* 2000;1477:189–214.
17. Weiner SJ, Kollman PA, Case DA, Singh UC, Ghio C, Alagona G, Profeta S, Weiner P. A new force field for molecular mechanical simulation of nucleic acids and proteins. *J Am Chem Soc* 1984;106:765–784.
18. Gasteiger J, Marsili M. Iterative partial equalization of orbital electronegativity—a rapid access to atomic charges. *Tetrahedron* 1980;36:3219–3228.
19. Kramer B, Rarey M, Lengauer T. Evaluation of the FlexX incremental construction algorithm for protein-ligand docking. *Proteins* 1999;37:228–241.